Natural variation in stomatal dynamics drives divergence in heat stress tolerance and contributes to the seasonal intrinsic water-use efficiency in *Vitis vinifera* (subsp. *sativa and sylvestris*)

Michele Faralli[1,*,§], Luana Bontempo[2], Pier Luigi Bianchedi[3], Claudio Moser[4], Massimo Bertamini[5,6], Tracy Lawson[7], Federica Camin[2,5,#], Marco Stefanini[4], Claudio Varotto[1,*]

[1]Department of Biodiversity and Molecular Ecology, Research and Innovation Centre, Fondazione Edmund Mach, via Mach 1, 38098 San Michele all'Adige (TN), Italy

[2]Department of Food Quality and Nutrition, Research and Innovation Centre, Fondazione Edmund Mach, via Mach 1, 38098 San Michele all'Adige (TN), Italy

[3]Technology Transfer Centre, Fondazione Edmund Mach, via Mach 1, 38010 San Michele all'Adige (TN), Italy

[4]Genomics and Biology of Fruit Crops Department, Research and Innovation Centre, Fondazione Edmund Mach, via Mach 1, 38098 San Michele all'Adige (TN), Italy

[5]Center Agriculture Food Environment (C3A), University of Trento, Via Mach 1, 38010 San Michele all'Adige, (TN), Italy

[6]Research and Innovation Centre, Fondazione Edmund Mach, via Mach 1, 38098 San Michele all'Adige (TN), Italy

[7]School of Life Sciences, University of Essex, Colchester, UK

* Authors to whom correspondence should be addressed. Email: michele.faralli@unitn.it; claudio.varotto@fmach.it

[§] Present address: Center Agriculture Food Environment (C3A), University of Trento, Via Mach 1, 38010 San Michele all'Adige, (TN), Italy

[#] Present address: International Atomic Energy Agency, Vienna International Centre, PO Box 100, A-1400 Vienna, Austria.

Highlight: Stomatal behavior can play a critical role in leaf thermoregulation and water conservation in grapevine when light and vapor pressure deficit are changing rapidly

Abstract

Stomata control CO_2 uptake for photosynthesis and water loss through transpiration, thus playing a key role in leaf thermoregulation, water-use efficiency ($_{i}WUE$) and plant productivity. In this work, we investigated the relationship between several leaf traits and hypothesized that stomatal behavior to fast (i.e. minutes) environmental changes co-determines along with steady-state traits the physiological response of grapevine to the surrounding fluctuating environment over the growing season. No relationship between $_{i}WUE$, heat stress (HS) tolerance and stomatal traits was observed in field grown grapevine, suggesting that other physiological mechanisms are involved in determining leaf evaporative cooling capacity and the seasonal ratio of CO_2 uptake (A) to stomatal conductance (g_s). Indeed, cultivars that in the field had an unexpected combination of high $_{i}WUE$ but low sensitivity to thermal stress, displayed a quick stomatal closure to light, but a sluggish closure to increased vapor pressure deficit (VPD) levels. This strategy aiming both at conserving water under a high-to-low light transition and in prioritizing evaporative cooling under a low-to-high VPD transition, was mainly observed in Regina and Syrah. Moreover, cultivars with different known responses to soil moisture deficit or high air VPD (isohydric vs anisohydric) had opposite behavior under fluctuating environments, with the isohydric cultivar showing slow stomatal closure to reduced light intensity but quick temporal responses to VPD manipulation. We propose that stomatal behavior to fast environmental fluctuations can play a critical role on leaf thermoregulation and water conservation under natural field conditions in grapevine.

Keywords: Grapevine; *Vitis vinifera*; stomatal dynamics; heat stress; genotypic variation; carbon isotope discrimination

Introduction

Climate change is increasing the need to select more resilient crop varieties to extreme weather conditions such as high temperature and reduced soil water availability (Mosedale *et al*., 2016; Henry, 2019). Grapevine (*Vitis vinifera* L.) is commonly considered well adapted to dry and hot environments, although a large body of evidence suggests significant detrimental roles of several abiotic stresses on phenology (Alikadic *et al*., 2019), quality (Pons *et al*., 2017), yield (Levin *et al*., 2020) and physiological responses (Bertamini *et al*., 2021). While crop management techniques (e.g. partial root-zone drying (Romero *et al*., 2012), deficit irrigation (Keller *et al*., 2016), Kaolin application (Frioni *et al*., 2019)) and the delivery of adapted rootstocks with potential preferable responses under specific disadvantageous conditions (Faralli *et al*., 2020; Frioni *et al*., 2020) have been shown to be effective at mitigating the negative effect of climate change on grapevine, further experimental evidence focusing at dissecting preferable traits for stress tolerance is needed. Indeed, extensive research has recently focused on grapevine responses to environmental stresses (Ferrandino *et al*., 2014; Venios *et al*., 2020). However, while this provided useful information regarding the mechanisms controlling the stress response, information regarding natural variation for key traits is scant in the literature. For instance, natural variation in photosynthesis, leaf morphology, xylem morphology, stomatal anatomy have been previously reported in several species such as wheat (Faralli *et al*., 2020; Driever *et al*., 2014), rice (Oshumi *et al*., 2007), cotton (Lu *et al*., 1998) and biomass crops (Faralli *et al*., 2021). These studies can open up the possibility to either detect the genomic regions controlling the trait of interest (van Bezouw *et al*., 2019) or hypothesize ideotypes with optimal combinations of traits for specific environments (Senapati *et al*., 2019).

Leaf transpiration and CO_2 uptake for photosynthesis are crucial processes in plants and primarily governed by stomata (Lawson & Blatt, 2014; Faralli *et al*., 2019; Faralli and Lawson, 2020). Indeed, carbon uptake and water loss are intrinsically linked by a trade-off between growth and water conservation mainly controlled by stomatal distribution, size and regulation that significantly impacts seasonal intrinsic water-use efficiency (Dittberner *et al*., 2018). Diversity in plant communities and survival rates have been previously shown to be shaped by stomatal regulation and density (McDowell *et al*., 2008), stressing the central role that stomata are playing in plant stress physiology. For instance, a significant positive relationship between stomatal density and stomatal conductance (g_s) has been previously reported in several species (Faralli *et al*., 2019; Franks *et al*., 2015; Franks and Beerling 2009). Similarly, reducing stomatal density through transgenic approaches yielded higher intrinsic water-use efficiency and enhanced water conservation in crop species (Caine *et al*., 2019; Dunn *et al*., 2019; Hughes *et al*., 2017). However, some studies on a range of species

(McAusland *et al*., 2016) including rice and vegetable crops (Bakker, 1991) did not provide evidence for stomatal conductance driven mostly be stomatal density. Indeed, stomatal size (SS), although less studied compared with SD, also plays a primary role on gas-exchange mainly owing to the negative and not linear relation that SS has with SD (Franks and Beerling 2009). Variation in SS also affects stomata regulation, with large SS associated with slow stomatal rapidity under dynamic conditions (Drake *et al*., 2013; McAusland *et al*., 2016). Since stomatal regulation is an order of magnitude slower than photosynthetic responses (Lawson & Blatt, 2014; Lawson and Vialet-Chabrand 2019), sluggish stomatal responses result in an unnecessary water loss under e.g. high-to-low light transition while negatively impacting CO_2 uptake when leaves are exposed to fast low-to-high light transition (Lawson and Blatt, 2014). The presence of natural variation in dynamic stomatal responses have been already proposed in few crops and speedy stomata hypothesized as a preferable trait to optimize CO_2 uptake and water-use efficiency under dynamic environmental conditions (Lawson *et al*., 2010; Lawson and Blatt, 2014; Durand *et al*., 2019). However, to our knowledge, there are no reports for natural variation in speed of stomatal responses to light and the association with heat stress tolerance and $_iWUE$ in grapevine.

A large body of studies focused on determining grapevine natural variation for important quantitative traits such as bunch compactness (Tello *et al*., 2015), disease resistance (Cadle-Davidson, 2008) or berry anthocyanin content (Fournier-Level *et al*., 2009) while only a handful of studies provide information regarding natural variation for key traits related to stomatal anatomy and functional stress tolerance (e.g. Kadir, 2006; Bartlett and Sinclair, 2021). For instance, in Coupel-Ledru *et al*., (2016) grapevine genotypes with higher leaf transpiration also showed higher stomatal density. Although stomatal density may show significant phenotypic plasticity to a series of environmental stimuli (e.g. CO_2, soil and air temperature) (Bertolino et al. 2019), the authors suggested that the number of stomata significantly contributed to variability in transpiration found in the grapevine mapping population and potentially water stress adaptation. Other reports provided further evidence of a tight relationship between heat tolerance and leaf evaporative cooling (i.e. transpiration rates) in grapevine (Venios *et al*., 2020). Indeed, when a shift in the balance between supply and demand of water is present, e.g. high VPD moves the hydraulic equilibrium towards demand, stomata respond to increased transpiration rate by reducing aperture, potentially via ABA accumulation (Soar *et al*., 2006). This behavior has been shown to exist in both anisohydric (low stomatal control) and isohydric (high stomatal control and water status maintenance) grapevine cultivars with the latter characterized by high concentrations of ABA in the xylem sap and therefore a more pronounced restriction in transpiration at high VPD (Soar *et al*., 2006). Transpiration sensitivity to VPD has been extensively proposed as an

important water-saving strategy in crops although, in grapevine, reduced sensitivity to VPD was considered as a strategy to minimize heat stress damage (Soar *et al*., 2009). While this behavior has been investigated in grapevine on a daily-hourly basis (Sade *et al.*, 2012; Soar *et al*., 2009), the response to fast environmental stimuli (e.g. changes in VPD in seconds, often occurring due to self-shading, sun cover etc.) has never been shown in grapevine, and no link between water loss, heat stress tolerance and rapid adjustment of stomata to fast VPD changes investigated in a large panel of varieties.

In this work we phenotyped a collection of *Vitis vinifera* subspecies *sativa* and *sylvestris* genotypes for stomatal, isotopic and chlorophyll fluorescence traits under different temperatures in a field trial. A subset of six genotypes were then grown in the greenhouse for subsequent assessments under dynamic light and VPD conditions. In Experiment 1 (field experiment) we test the hypothesis that i) a broad phenotypic variation is present in *Vitis* for the trait analyzed,ii) variation exist for key traits between *sativa* and *sylvestris* and iii) a positive relationship exist between *¡WUE* and heat stress (HS) sensitivity. The objective of the subsequent experiments in semi-controlled environmental conditions were to i) assess the variation for stomatal rapidity in a subset of genotypes and ii) to determine the presence of a relationship between stomatal dynamic responses and field *¡WUE.*

Materials and methods

Experiment 1: field experiment

The experiment was conducted in summer 2020 and the list of *Vitis* genotypes used is shown in Supplementary table 1. For each genotype, five plants were available for analysis (n=5). The genotypes belong to the FEM grape germplasm collection (ITA362), located in San Michele all'Adige, Italy (46° 10' 53" N, 11° 7' 2" E). All plants were grafted on the rootstock Kober 5BB (a rootstock with medium vigour commonly used in north Italy) in five replicates (thus clones) per genotype and trained according to the Guyot system. The vineyard was planted in 2004 in a flat field and genotypes (5 replicates each) were assigned into one of the five field plots available. The vineyard has south exposure with a calcareous skeletal soil (pH 7.9), a sandy-loam texture (sand 52.5%, loam 41.9%, 5% clay), low organic substance and a balanced content of nutritive elements. Density of planting was 5600 plants ha^{-1}. Temperature and rainfall were monitored with a weather station 50 m away from the field site and are shown for the whole 2020 in Supplementary Figure 1. Field management was uniform for all the genotypes and it followed standard agronomic techniques of the Trentino region.

Experiment 2: greenhouse experiment

The experiment was conducted between December and April 2021 while plant material for greenhouse growth was collected in the field in December 2020. Six genotypes were selected for contrasting traits according to Experiment 1: Cabernet Sauvignon, Syrah, Teroldego, Regina, Sinni and Ketsch. Briefly, cuttings were produced from field branches (n=25) on the 18 December 2020 and placed at 4°C under dark for ten days. The length of each cutting was standardized at around 25 cm (i.e. only branches with similar internode lengths were used) and only one apical bud was left to burst. Subsequently, cuttings were placed under water and moved to a controlled environment growth cabinet at 30°C and 90% relative humidity to induce budburst. On the 29 January 2021, after the application of a solution of Indole-3-butyric acid to the basal bud, cuttings were transferred in 1.3L pots all containing the same amount of growing substrate (600g of TerCompost ExtraQuality Professional, Tercomposti Spa, Calvisano, Italy—a mixture of peat, perlite and pumice). Pots were then moved to a semi-controlled environment greenhouse under natural light conditions with supplementary light of 200 µmol m^{-2} s^{-1} on average (14/10 day/night photoperiod). Plants were irrigated with an automatic watering system allowing saturating conditions every two days and pruned to one shoot only. Temperature and relative humidity were monitored with a data logger (Tinytag) every hour while total light radiation was recorded with a pyranometer mounted above the greenhouse. Data are provided in Supplementary Figure 2

Stomatal anatomy and g_{max} calculation

Stomatal analysis was carried out both in Experiment 1 and 2. In Experiment 1 a phenotyping experiment was carried out and for all the 49 genotypes stomatal impressions were carried out with viscous nail polish (one shoot in n=5 plants per genotype) as shown in Meeus et al. (2020). Impressions (around 2.5 cm^2) were taken on the lateral lobes and avoiding the main veins and each leaf used for the analysis (5^{th} leaf fully-expanded of a west-exposed branch) was tagged. Impressions made were subsequently placed onto microscope slide via clear adhesive tape. In Experiment 2, the same protocol for impression collection was used (n=5) onto the 7^{th} fully expanded leaf for each genotype used. Images were taken on a light microscope (DM2005, Leica Microsystems, Wetzlar, Germany) mounted with a camera (Leica Microsystems). Stomatal density (SD) was assessed with ImageJ and subsequent standardization to mm^{-2} was carried out. All the genotypes were strongly hypostomatic (no presence of stomata on adaxial leaf surface) and therefore the data presented in this work focused on abaxial stomata only. Complex size (i.e. pore and stomatal length and width) was manually measured in ImageJ from a total of 15 stomata

from each genotype, taken from five biological replicates. Pore area and stomatal size (SS) were calculated as an ellipse and the measured length treated as major axis while the measured width as the minor axis. Maximum pore aperture was calculated as an ellipse from axes equal to the measured aperture length and half of the aperture width. Pore depth (*l*) was taken as equal to guard cell width at the center of the stoma. Anatomical g_{max} was calculated using the Franks and Beerling (2009) equation:

$$g_{max} = \frac{\frac{d}{v} \cdot SD \cdot a_{max}}{l + \frac{\pi}{2}\sqrt{a_{max}/\pi}}$$

Where *SD* is stomatal density, l is pore depth, a_{max} the maximum area of the open stomatal pore and approximated as $\pi(PL/2)^2$ (*PL*, stomatal pore length), *d* (0.0000249 m^2 s^{-1}) is the diffusivity of water in air and *v* (0.0245 m^3 mol^{-1}) is the molar volume of air.

Chlorophyll fluorescence

Chlorophyll fluorescence analysis was carried out in Experiment 1 and 2 with a portable fluorescence system (HandyPEA, Hansatech, Kings Lynn, UK). In the field, data of maximum quantum yield of photosystem II in dark adapted samples (F_v/F_m) were collected in early morning and afternoon. Leaves in the same branch used for stomatal analysis (6th or 7th leaf in one shoot for n=5 plants per genotype) were dark adapted by using leaf clips for 45 minutes. The analyses were carried out on the 28th and 30th July 2020 when most of the genotypes were around veraison. Leaves were analyzed in early morning (from 5:00 to 8:00) and treated as control data (average air temperature of 22.4±1.6°C). Measurements were repeated in the afternoon between 14:00 and 17:00 and considered as heat stressed (average air temperature of 33.2±0.5°C). Data collection was randomized to avoid time effect. Reduction in F_v/F_m was calculated as the difference between the control and the heat stressed F_v/F_m value for each individual and expressed as percentage.

During Experiment 2 chlorophyll fluorescence analysis was carried out in detached leaves (8th to 9th leaf in the main branch) and subjected to a controlled increase in air temperature inside a controlled environment chamber. Leaves (n=6 per genotype) were collected in the greenhouse, placed in tubes containing deionized water and immediately moved to the laboratory. Petioles were immediately re-cut under water and samples were placed in test tubes containing fresh de-ionized water and moved to a growth chamber (Model BD 56, BINDER GmbH,Tuttlingen, Germany) under dark and at 25°C temperature for 1h. Leaf clips for dark adaptation were positioned on the sampled leaves. The heat stress treatment was applied the same day and consisted on a step-wise increase of 3°C in air temperature every 15 minutes (from 25°C to 52°C, 10 steps in total). The maximum quantum yield of

photosystem II in dark adapted samples (F_v/F_m) was recorded for each leaf after a period of 15 minutes of stabilization at each temperature applied.

Isotopic analysis

Carbon and nitrogen stable isotope ratio analysis was carried out in Experiment 1. Sampling was carried out in the same day and around postveraison as it has been shown to be a good estimate of the integral intrinsic water-use efficiency (Bchir *et al.*, 2016). Mature leaves from the same branch used for stomatal and fluorescence analyses were collected and placed immediately in an oven at 80°C for 48 hours to allow complete dehydration. $\delta^{13}C$ and $\delta^{15}N$ were analyzed in 2 mg aliquotes of leaf samples weighted in tin capsules. Samples were combusted in an elemental analyzer (Thermo Flash EA 1112 Series, Bremen, Germany), CO_2 was separated by chromatography and directly injected into a continuous-flow isotope ratio mass spectrometer (Thermo Finnigan Delta V, Bremen, Germany) through the interface ConFlo IV dilutor device (Thermo Finningan, Bremen, Germany). Samples were measured in duplicate. The isotope ratios were expressed in δ‰ against Vienna-Pee Dee Belemnite for $\delta^{13}C$ and air for $\delta^{15}N$ according to the following equation:

$$\delta‰ = \frac{R_{SA} - R_{REF}}{R_{REF}}$$

where R_{SA} is the isotope ratio measured for the sample and R_{REF} is the international standard isotope ratio. The isotopic values for $\delta^{13}C$ and $\delta^{15}N$ were calculated through the development of a linear equation against working in-house standards, which were themselves calibrated against international reference materials: potassium nitrate IAEA-NO3 (IAEA-International Atomic Energy Agency, Vienna, Austria) for $^{15}N/^{14}N$, L-glutamic acid USGS 40 (U.S. Geological Survey, Reston, VA, USA) for $^{13}C/^{12}C$ and $^{15}N/^{14}N$, fuel oil NBS-22 and IAEA-CH-6 for $^{13}C/^{12}C$. For $\delta^{13}C$ and $\delta^{15}N$ the uncertainty of measurement (calculated as one standard deviations) was 0.1‰ and 0.2‰, respectively.

Gas-exchange protocols

Gas-exchange analysis was carried out in Experiment 2 under controlled environment conditions. All the data were collected with a Li-Cor 6400 (Li-Cor, Lincoln, NE,USA) with an integrated fluorescence leaf cuvette (LI-6400-40; Li-Cor). To evaluate the temporal response of stomatal conductance (g_s) of the six genotypes chosen to dynamic light conditions, a step-change in light protocol was carried out (n=5). Briefly, between 800 and 1400 plants were moved from the greenhouse prior to analysis and acclimated to the climate-controlled room

(20°C and 60%RH on average) for 30 minutes. Subsequently, the 7th leaf from the base of the plant (for all the plants, the 7th leaf represented the fully-expanded leaf) for each genotype was clamped into the LiCor cuvette and first equilibrated at a near-saturating photosynthetic photon flux density (PPFD) of 1000 µmol m^{-2} s^{-1} until both CO_2 assimilation rate (A) and stomatal g_s reached 'steady state,' defined as a ~2% maximum change in rate during a 10 min period (generally 60 min). After equilibration, PPFD was reduced to 100 µmol m^{-2} s^{-1} for 1 h. Data were logged every minute. The conditions inside the leaf cuvette were kept constant at 25 ± 0.1°C leaf temperature, at VPD of 1.5 kPa and at 400 µmol CO_2 mol^{-1} air (ambient CO_2 concentration, C_a). To evaluate the temporal response of g_s to rapid changes in vapor pressure deficit (VPD) conditions, a step-change in VPD protocol was carried out. Acclimation was carried out as for light step-changes and the 7th leaf for each genotype was clamped into the LiCor cuvette and first equilibrated at an average VPD of 1.5 kPa. After equilibration, RH inside the cuvette was reduced from 70 to 10% and VPD was kept constant to 3.5 kPa on average for 1h. Data were logged every minute. The conditions inside the leaf cuvette were kept constant at 30 ± 0.1◦C leaf temperature, at a near-saturating PPFD of 1000 µmol m^{-2} s^{-1} and and at 400 µmol CO_2 mol^{-1} air (ambient CO_2 concentration, C_a). CO_2 assimilation rate at saturating light (A_{sat}), stomatal conductance at saturating light (g_{sat}), intrinsic water-use efficiency ($_iWUE$, A_{sat}/g_{sat} ratio) and delta g_s (difference between g_{sat} and g_s after 1h of protocol) were estimated from step-changes in light curves and mentioned as steady-state parameters. Curves of g_s to time (minutes) were subsequently analyzed with a log decay fitting ($g_s = (g_{s0} - Plateau) \cdot e^{(-K*Time)} + Plateau$). T50 is expressed in the time units of the X axis and represents the time to reach 50% of stomatal closure following either low light or high VPD.

Statistical analysis

All data were analyzed with Rstudio. Data were checked for normality and residuals vs fitted value and all the physiological traits were analysed with a one– or two-way analysis of variance (ANOVA) (depending on factor number) via the aov function. All the graphs were produced with ggplot2. Correlations were carried out with the ggcorr package. Curve fitting was analyzed for dynamic responses as above. Associations between traits were assessed via linear regression and Pearson test. When present, Fisher's test was used for multiple comparison while t-test was used for two-group comparisons.

Results

Experiment 1

Significant variation ($p<0.001$) was observed in anatomical stomatal traits analyzed in Experiment 1 (Figure 1). Mean stomatal density per mm^{-2} on the abaxial surface ranged from 83.8 ± 8.7 (Fethiye 56-64) to 176.2 ± 8.3 (Albariño) (Supplementary Table 2). Stomata were not observed on the adaxial surface for all the genotypes. When grouped by sub-species, there was no significant difference in stomatal density between *sativa* and *sylvestris*. On the contrary, significant variation was observed between *sativa* and *sylvestris* in stomatal size ($p<0.001$) with *sativa* showing greater size than *sylvestris* while significant variation was observed for all the cultivars with stomatal size ranging from 400 to 1000 μm^2. There were no differences ($p=0.139$) for anatomical g_{max} between subspecies, although a significant variation was observed between genotypes (i.e. both *sativa* and *sylvestris*) for g_{max} ranging from 1.2 ± 0.06 to 3.0 ± 0.08 mol m^{-2} s^{-1}.

Significant variation ($p<0.001$, $p=0.001$ for reduction in F_v/F_m) was observed for functional leaf traits analyzed in the field. The reduction in F_v/F_m under heat stress compared to the control was 10.6% on average with significant variation between genotypes ($p=0.001$), while the difference between subspecies was not significant ($p=0.563$). Intrinsic water-use efficiency assessed through $\delta^{13}C$ highlighted a significant variation ($p=0.024$) between subspecies, with *sativa* being more efficient at using water than *sylvestris*. Genotypic variation for $\delta^{13}C$ was significant ($p<0.001$). $\delta^{15}N$ significantly varied between genotypes ($p<0.001$) and subspecies ($p<0.001$).

Correlations between traits (Figure 2A) show positive and significant ($p<0.001$) associations between g_{max} and stomatal density or size. In addition, stomatal size was positively correlated with $\delta^{15}N$ ($p<0.01$) and $\delta^{13}C$ ($p<0.05$). A significant ($p<0.05$) and positive relationship was also present between $\delta^{15}N$ and $\delta^{13}C$. No significant correlations were observed between stomatal size and density or heat sensitivity (reduction in F_v/F_m) and other anatomical and functional traits. In Figure 2B, a scatter plot of the average values between $\delta^{13}C$ and reduction in F_v/F_m is shown for the selected lines in Experiment 2. Some genotypes (Sinni and Cabernet Sauvignon, red circle) showed high *iWUE* and high sensitivity to heat stress while there were genotypes displaying low *iWUE* and limited sensitivity to high temperatures (light blue circle). Some genotypes showed high *iWUE* followed by low sensitivity of PSII to thermal stress (e.g. Teroldego and Regina, black circles). These lines with such a contrasting combination of $\delta^{13}C$ and reduction in F_v/F_m under heat stress were chosen for Experiment 2.

Experiment 2

Stomatal anatomical traits

Greenhouse assessment of stomatal anatomical features revealed significant differences between the selected genotypes in stomatal density ($p<0.001$), stomatal size ($p=0.004$) and anatomical g_{max} ($p<0.001$) (Figure 3). Stomatal densities in the greenhouse were generally lower than those in the field while stomatal sizes were similar, leading to a lower g_{max} for the genotypes assessed. Significant and positive correlations existed between greenhouse and field traits (Supplementary Figure 3) suggesting conserved phenotypes for different environmental conditions. In general, Ketsch and Cabernet Sauvignon showed the highest stomatal densities while Syrah and Regina the lowest. Stomatal size was higher in Teroldego and Regina when compared to Cabernet Sauvignon and Sinni and this led to lower g_{max} in Regina and Syrah when compared to Cabernet Sauvignon, Teroldego and, in particular, Ketsch.

Stomatal kinetics following a step increase in irradiance

Steady-state gas-exchange traits at near-saturating light intensity highlighted significant variation for most of the traits analysed (Figure 4). Ketsch and Teroldego showed higher g_{sat} than Cabernet Sauvignon and Sinni ($p=0.011$) while no significant differences were observed for A_{sat} ($p=0.380$). On the contrary, a significant variation was observed for ${}_{i}WUE$ between lines with Sinni and Cabernet Sauvignon having higher ${}_{i}WUE$ than Regina, Ketsch and in particular Syrah ($p<0.001$). The difference between g_{sat} and steady-state g_s at low light (δg_s) showed a higher delta for Ketsch and Teroldego when compared to Syrah and Cabernet Sauvignon ($p=0.015$)

The dynamics of stomatal closure following a step change in light (1000 to 100 µmol m^{-2} s^{-1} PPFD) for all the genotypes are shown in Figure 5 along with the dynamic of ${}_{i}WUE$. The modeled log decay fitting is also shown (Figure 5G). There was a significant difference for time to reach 50% of stomatal closure ($T50$) ($p=0.022$, Figure 5H). In Cabernet Sauvignon, Sinni and Ketsch $T50$ was achieved between 15 and 20 minutes, while stomatal closure was faster in Teroldego, Syrah and Regina with an average $T50$ between 6 and 10 minutes.

Stomatal kinetics in response to changes in VPD

The fitted log decay function for each genotype and for average g_s values after a step-change increase in VPD (1.5 to 3.5 kPa) is shown in Figure 6A. There was a significant variation in the time to reach 50% of stomatal closure ($T50$) ($p=0.003$) with Sinni and Ketsch

being the slowest while all the *sativa* showed faster *T*50 (10 minutes on average). The absolute $g_{shighVPD}$ (g_s after one hour of high VPD treatment) show significant variation between genotypes (p=0.044) with Syrah and Regina showing higher g_s values (around 0.10 mol m^{-2} s^{-1}) than Cabernet Sauvignon and Sinni. This different sensitivity to VPD between cultivars led to lower limitation of CO_2 assimilation by g_s with higher reduction in A_{sat} for Cabernet Sauvignon than Syrah.

Discussion

In this study, we characterized forty-nine genotypes belonging to two *Vitis vinifera* subspecies under field conditions for several physiological traits. Our initial objective was to assess whether a relationship exists between *iWUE* estimated with carbon isotope discrimination and sensitivity to HS conditions. Under non-limiting water conditions, high transpiration rate can be a preferable trait to overcome heat waves (Venios *et al*., 2020). Since stomata are the main drivers of transpiration (Faralli *et al*., 2019), we hypothesized a higher sensitivity to HS (i.e. marked reduction in F_v/F_m as proposed in other species by Sharma et al. 2017) in genotypes with enhanced seasonal *iWUE* and that this relationship could be explained by differences in stomatal anatomical features. In addition, key genotypes were characterized under controlled conditions to assess whether dynamic responses to environmental cues may partially explain some of the variation found in the field for adaptive traits. Indeed, heat waves and prolonged conditions of HS are expected to increase in the near future and are already experienced by crops worldwide (Jagadish *et al*., 2021). Water conservation is a priority for agriculture although it can often lead to reduced leaf evaporative cooling and sub-optimal leaf temperature for photosynthesis (Faralli *et al*., 2019). Adaptive strategies to heat and drought have often been considered antithetical and dissecting preferable traits that may induce adaptation to combination of stresses is surely a priority that needs to be addressed, in particular in a valuable crop such as *V. vinifera*.

Variation exists between genotypes for anatomical and key adaptive steady-state traits in V. vinifera

In our study, large variation was observed in stomatal anatomical traits, which resulted in significant variation in g_{max}. Our results (SD ~100-200 stomata mm^{-2}, SS ~400-900 μm^{-2}) are in line with genotypic variation for stomatal anatomical traits observed in *Vitis* in previous work (Coupel-Ledru *et al*., 2016; Rogiers *et al*., 2009). Previous research has suggested a negative relationship between SD and SS, with decreasing SS with increasing SD (Franks *et al*., 2009; Dittberner *et al*., 2018). For instance in *Eucalyptus globulus,* anatomical g_{max} was constrained by the negative SS-SD relationship, and higher g_{max} were observed in a combination of low SS and high SD (Franks *et al*., 2009). Interestingly, this negative

association was linked to an improved economy of epidermal space allocation (Lawson and McElwain, 2016; Dow *et al*., 2014) and reversion back to smaller numbers of larger stomata was hypothesized as a better strategy for conditions in which lower g_{max} is required. On the contrary, smaller stomata have often been proposed to have faster responses to environmental stimuli potentially due to more rapid changes in solute concentrations associated to small guard cells (Lawson and Vialet-Chabrand, 2019). In our work there was no significant relationship between SD and SS in accordance with several recent studies in a range of species (e.g. McAusland *et al*., 2016; Eyland *et al*., 2021; Stevens *et al*., 2021) suggesting that plasticity in maximum stomatal conductance may not be constrained by the presence of a negative relationship in grapevine. However, while carbon dioxide (Lawson *et al*., 2002) and light intensity (Poole *et al*., 2000) are factors known to control the definite development of stomata and the spatial patterning over the leaf, interactions between temperature, humidity and soil moisture deficit can influence epidermal cells spacing (McElwain, 2004). This can result in different SD for a similar stomatal index (ratio of stomata to number of epidermal cells; Lawson et al., 2002). In our work, environmental conditions and vine management were similar for all the genotypes during the growing season and therefore the potential environmental effect or carbohydrate status on stomatal density is unlikely. However, genotypic variation for sensitivity to environmental cues may have influenced epidermal cells spacing in some genotypes, thus leading to altered SD with subsequent influences on gas-exchange per unit of leaf area.

A large variation for HS tolerance assessed as reduction of F_v/F_m between control and HS condition was observed between the cultivars. However, this variation was not explained by either stomatal size or density suggesting that i) leaf evaporative cooling is mainly determined by operational stomatal conductance and that ii) maximum anatomical conductance is a bad predictor of grapevine performances under developing stress conditions. Indeed, although anatomically possible, plants do not operate close to their g_{max} (McElwain *et al*., 2016) while their operating g_s instead usually remains at around 20% of their maximum capacity, which corresponds to the turgor pressure in which guard-cells can most efficiently control pore apertures (Dow *et al*., 2014). Indeed, carbon isotope discrimination analysis revealed an overall broad variation between genotypes with larger SS associated with higher $_i$*WUE*. Previous studies confirmed that larger SS (yet, somehow lower SD) induced lower g_{max} and therefore a more efficient use of water (Franks *et al*., 2009). However, in this study the correlation between carbon isotope discrimination and reduction in F_v/F_m was not significant, with several genotypes being both water-use efficient and heat stress tolerant. Restricted transpiration rates are generally found in genotypes with elevated sensitivity to VPD and water stress (so-called isohydric behavior). For instance, some genotypes, e.g. Syrah and Cabernet Sauvignon, showed either low $_i$*WUE* and

elevated tolerance to HS (Syrah) or high $_iWUE$ but significant F_v/F_m reductions under developing HS. This behavior was also corroborated by gas-exchange analysis, in which Syrah showed a high g_{sat} compared with Cabernet Sauvignon. The anisohydric and water-spender behavior was already proposed in previous studies where Syrah showed a non-conservative response to increasing VPD levels or water stress (Soar *et al*., 2009). Similarly, Cabernet Sauvignon showed a tight stomatal control under developing water stress, putatively modulated by either ABA sensitivity or hydraulic traits (e.g. xylem vessels diameter). This wide phenotypic variation can be exploited in breeding programs focusing at enhancing grapevine adaptation to environmental stresses and may assist management decision for physiological fine-tuning under disadvantageous conditions.

Domestication and breeding increased $_iWUE$, yet enhancing stomatal size and maintaining high g_s under low light conditions

Vitis vinifera subsp. *sativa* has been a source of food and wine since its hypothesized domestication ~8.0 kya from its wild progenitor, *V. vinifera* subsp. *sylvestris*. Advances have been focusing at understanding grapevine evolutionary domestication, with Zhou *et al*., (2017) showing that in cultivated grapes, candidate-selected genes were identified for sugar metabolism, flower development, and stress responses while candidate-selected genes in the wild sample were limited to abiotic and biotic stress responses. However, in our work, *V. vinifera* subsp. *sativa* showed higher $_iWUE$ than subsp. *sylvestris*, suggesting that crop improvement led to a more careful use of water during the growing season. The increase in $_iWUE$ was also accompanied by increases in stomatal size and generally higher g_s values under low light conditions. Increasing stomatal size should yield higher g_{max} hence reducing $_iWUE$, at least under steady-state conditions. Similarly, higher g_s values under low light conditions should increase water loss from the leaf followed by limited photosynthetic capacity. However, these traits in subsp. *sativa* were accompanied by a generally higher sensitivity (i.e. faster stomatal closure) to increasing VPD levels than subsp. *sylvestris*, suggesting that a fast restricted transpiration to high evaporative demand was either i) an unintentional trait selected with breeding or ii) a strategy resulting from the domestication process. VPD response in grapevine have been associated with ABA metabolism, with cultivars displaying a conservative response to VPD also showing higher ABA levels in xylem sap and leaf during daily developing increases in VPD although passive hydraulic VPD response has been also hypothesized (Merilo *et al*., 2018). In general, subsp. *sylvestris* seems to be less conservative under developing VPD, suggesting that leaf evaporative cooling and *A* maintenance are prioritized under fast transition from low to high VPD. When plants were subjected to high to low light transition, a similar behavior was observed (apart from Cabernet Sauvignon) with subsp. *sylvestris* showing slower stomatal closure than

subsp. *sativa*. Sluggish stomatal responses to fluctuating light intensities can reduce seasonal $_{i}WUE$ following a substantial water loss for a limited CO_2 fixed (Lawson & Blatt, 2014; Lawson & Vialet Chabrand 2019; Vialet-Chabrand *et al*., 2017; Matthews *et al*., 2018). In rice, genotypes with fast stomatal closure under high to low light transition had higher $_{i}WUE$ and lower biomass penalties under reduced water availability (Qu *et al*., 2016) suggesting that stomatal dynamics under fluctuating light is an important component of drought tolerance and soil moisture conservation. Therefore, our data show that a series of preferable traits were selected in subsp. *sativa* (high g_s at low light, greater stomatal size, fast stomatal closure under low light and VPD) in particular related to a more careful water-use behavior under dynamic field conditions yet maintaining high steady-state values.

Preferable combination of responses to light (fast) and VPD (slow) is present in genotypes with greater HS tolerance and high $_{i}WUE$

Speed of stomatal responses to fluctuating environmental conditions is an underrated physiological trait with potential for contribution to future crop improvement. However, while variation has been shown in a few crop species (McAusland *et al.*, 2016; Eyland *et al*., 2021; Acevedo-Siaca *et al*., 2021, Faralli *et al*., 2019), to our knowledge, this is the first report presenting phenotypic variation in g_s for rapid variation in VPD and light levels in grapevine. One of the most interesting output of this work is the significant genotypic variation observed for g_s responses under different environmental stimuli (in this case, VPD and light intensity) and that these contrasting behaviors partially explained the unexpected performance under HS of some cultivars with high $_{i}WUE$.

Stomatal closure to reduced light intensity is mainly governed by the ion transport across the plasma membrane and tonoplast, and increasing guard cell volume to surface ratio has been associated to an increased time to adjust solute content within the cell volume (Lawson and Blatt, 2014). Indeed, often, speed of stomatal responses to light were linearly correlated with stomatal anatomical features and smaller stomata were frequently exhibiting fast g_s responses (Hetherington and Woodward, 2003). In some species, however, this correlation was not observed and in rice, larger stomata had faster A and g_s induction than smaller stomata (Zhang *et al*., 2019). In our work, no significant association was observed between anatomical traits and speed of stomatal closure to light, while a significant negative correlation (p=0.026) was observed between g_{smin} and $T50$ (i.e. genotypes with higher g_{smin} had faster g_s induction) (Supplementary Figure 4). Similarly, a positive correlation was present between δg_s and $T50$ (p=0.045), overall suggesting that faster stomatal responses were present in cultivars with a higher g_{smin}. Previous work on woody plants (Meinzer *et al*., 2017) showed that anisohydric species responded rapidly to light accompanied by generally lower $_{i}WUE$ than isohydric species and similar results were observed in other species

(Barratt *et al*., 2021). Indeed, for *Vitis vinifera* subsp. *sativa*, Cabernet Sauvignon, a commonly so-called isohydric cultivar, had high steady-state $_{i}WUE$ yet slow stomatal closure while the opposite was observed in Syrah. This clearly corroborates the opposite behavior for seasonal $_{i}WUE$ between Syrah and Cabernet Sauvignon, with the latter showing a pronounced $_{i}WUE$ majorly explained by low steady state g_s values, slow responses to light but high sensitivity to VPD.

Assuming transpiration as the main driver of leaf heat dissipation, seasonal $_{i}WUE$ should be negatively correlated with evaporative cooling and g_s while a positive association is expected between $_{i}WUE$ and reduction of F_v/F_m under developing HS. However, this relationship was not significant between field and greenhouse datasets, while *T*50 was negatively correlated with $\delta^{13}C$, and positively with reduction in F_v/F_m (Figure 7). Similarly, $_{i}WUE$ was positively associated with $\delta^{13}C$ and $g_{shighVPD}$ negatively associated with reduction in F_v/F_m. Regina and Syrah had quick responses to light and slow responses to VPD, suggesting that dynamic responses were the main drivers of seasonal $_{i}WUE$ with these varieties potentially showing desirable dynamic traits. Rapid stomatal closure in Regina under a high to low light transition may be the cause of an enhanced seasonal $_{i}WUE$ and, coupled with an insensitivity to VPD and a maintenance of high g_s at high VPD levels, explains the relatively low reduction in F_v/F_m under field conditions. Indeed, in dark adapted and detached leaves, the range of F_v/F_m reduction for the different cultivars was not maintained (Supplementary Figure 5). Similarly, as already partially reported in the literature (Soar *et al*., 2006; Soar *et al*., 2009) Syrah was characterized by a quick g_s reduction under fluctuating light, high steady-state g_s, and limited sensitivity to fast changes in VPD. In the field, these behaviors can prioritize either $_{i}WUE$ and evaporative cooling depending on the stressor at which the plants are subjected and therefore better optimizing gas-exchange in short time-frames. The trends observed in this work should be additionally validated in the field where the time-course of canopy temperature and leaf water status may help dissecting potentially contrasting strategies between genotypes and cultivars x rootstock combinations. Indeed, further work should focus at determining the underlying mechanisms of speedy stomata in grapevine, understanding the interaction with standard grapevine management approaches such as irrigation and link these preferable traits with rootstock-scion physiology.

Conclusions

Our field screening provides a large physiological characterization for several traits in *Vitis vinifera* and shows the presence of a wide phenotypic variation both in *sativa* and in *sylvestris* subspecies. We also observed for the first time that a series of desirable traits (e.g. higher stomatal size and high $_{i}WUE$) were present in subsp. *sativa* when compared to subsp. *sylvestris*, suggesting that unintentional selection for $_{i}WUE$ has been carried out,

potentially as a result of domestication. However, in natural field conditions, leaf overlapping and cloud cover impose fast changes in light and VPD levels; suboptimal stomatal adjustment can lead to nonsynchronous behavior between *A* and g_s, which can result in reduced *¡WUE* and lowered leaf evaporative cooling under high temperature conditions. Our data for the first time show that preferable combination of traits for optimizing gas-exchange under natural field conditions are present in *Vitis vinifera* subsp. *sativa*. In particular, Regina was characterized by high seasonal *¡WUE* despite a relatively high steady-state g_s, potentially owing to a capacity to quickly react to fluctuating light conditions. Yet, reduced stomatal sensitivity to fast increasing VPD levels may maintain leaf heat dissipation and optimal leaf temperature for photosynthesis (i.e. Syrah), thus enhancing heat tolerance under the natural fluctuating environmental conditions. We propose that stomatal behavior to fast changes in light and VPD can play a critical role in leaf thermoregulation and water conservation in grapevine.

Acknowledgments

We thank Davide Stragliotto for helping with data collection in the field. We thank Damiano Gianelle for lending the Licor6400, Elena Gottardini for lending the chlorophyll fluorescence systems and Monica Tolotti for the use of the microscope.

Author contributions

MF, CV and MS designed the experiments. MF collected and analyzed all the data. MF wrote the manuscript. LB and FC carried out isotopic measurements. PLB helped with field sampling and plant growth during the greenhouse experiments. TL, CM and MB helped with data interpretation. All the authors approved the final version of the manuscript.

Data availability

All data supporting the findings of this study are available within the paper and within its supplementary materials published online.

References

Acevedo-Siaca LG, Dionora J, Laza R, Paul Quick W, Long SP. 2021. Dynamics of photosynthetic induction and relaxation within the canopy of rice and two wild relatives. Food and Energy Security, e286.

Alikadic A, Pertot I, Eccel E, Dolci C, Zarbo C, Caffarra A, ... and Furlanello C. 2019. The impact of climate change on grapevine phenology and the influence of altitude: A regional study. Agricultural and forest meteorology 271, 73-82.

Bakker JC. 1991. Effects of humidity on stomatal density and its relation to leaf conductance. Scientia Horticulturae 48, 205-212.

Barratt GE, Sparkes DL, McAusland L, Murchie EH. 2021. Anisohydric sugar beet rapidly responds to light to optimize leaf water use efficiency utilizing numerous small stomata. AoB Plants 13, plaa067.

Bartlett MK, Sinclair G. 2021. Temperature and evaporative demand drive variation in stomatal and hydraulic traits across grape cultivars. Journal of Experimental Botany 72, 1995-2009.

Bchir A, Escalona JM, Gallé A, Hernández-Montes E, Tortosa I, Braham M, Medrano H. 2016. Carbon isotope discrimination (δ13C) as an indicator of vine water status and water use efficiency (WUE): looking for the most representative sample and sampling time. Agricultural Water Management 167, 11-20.

Bertamini M, Faralli M, Varotto C, Grando MS, Cappellin L. 2021. Leaf Monoterpene Emission Limits Photosynthetic Downregulation under Heat Stress in Field-Grown Grapevine. Plants 10, 181.

Bertolino LT, Caine RS, Gray JE 2019. Impact of stomatal density and morphology on water-use efficiency in a changing world. Frontiers in Plant Science, 10, 225.

Cadle-Davidson L. 2008. Variation within and between Vitis spp. for foliar resistance to the downy mildew pathogen Plasmopara viticola. Plant disease 92, 1577-1584.

Caine RS, Yin X, Sloan J, Harrison EL, Mohammed U, Fulton T, ... Gray JE. 2019. Rice with reduced stomatal density conserves water and has improved drought tolerance under future climate conditions. New Phytologist 221, 371-384.

Coupel-Ledru A, Lebon E, Christophe A, Gallo A, Gago P, Pantin F, ... Simonneau T. 2016. Reduced nighttime transpiration is a relevant breeding target for high water-use efficiency in grapevine. Proceedings of the National Academy of Sciences 113, 8963-8968.

Dittberner H, Korte A, Mettler-Altmann T, Weber AP, Monroe G, de Meaux J. 2018. Natural variation in stomata size contributes to the local adaptation of water-use efficiency in Arabidopsis thaliana. Molecular ecology 27, 4052-4065.

Drake PL, Froend RH, Franks PJ 2013. Smaller, faster stomata: scaling of stomatal size, rate of response, and stomatal conductance. Journal of experimental botany 64, 495-505.

Driever SM, Lawson T, Andralojc PJ, Raines CA, Parry MAJ 2014. Natural variation in photosynthetic capacity, growth, and yield in 64 field-grown wheat genotypes. Journal of experimental botany, 65, 4959-4973.

Dow GJ, Bergmann DC, Berry JA. 2014. An integrated model of stomatal development and leaf physiology. New Phytologist 201, 1218-1226.

Dunn J, Hunt L, Afsharinafar M, Meselmani MA, Mitchell A, Howells R, ... Gray JE. 2019. Reduced stomatal density in bread wheat leads to increased water-use efficiency. Journal of experimental botany 70, 4737-4748.

Durand M, Brendel O, Buré C, Le Thiec D. 2019. Altered stomatal dynamics induced by changes in irradiance and vapour-pressure deficit under drought: impacts on the whole-plant transpiration efficiency of poplar genotypes. New Phytologist 222, 1789-1802.

Eyland D, van Wesemael J, Lawson T, Carpentier S. 2021. The impact of slow stomatal kinetics on photosynthesis and water use efficiency under fluctuating light. Plant Physiology 186, 998-1012.

Faralli M, Lawson T. 2020. Natural genetic variation in photosynthesis: an untapped resource to increase crop yield potential? The Plant Journal 101, 518-528.

Faralli M, Bianchedi PL, Bertamini M, Varotto C. 2021. Rootstock Genotypes Shape the Response of cv. Pinot gris to Water Deficit. Agronomy 11, 75.

Faralli M, Matthews J, Lawson T. 2019. Exploiting natural variation and genetic manipulation of stomatal conductance for crop improvement. Current opinion in plant biology 49, 1-7.

Faralli M, Williams K, Corke F, Li M, Doonan JH, Varotto C. 2021. Interspecific and intraspecific phenotypic diversity for drought adaptation in bioenergy Arundo species. GCB Bioenergy 13, 753-769.

Ferrandino A., Lovisolo C. 2014. Abiotic stress effects on grapevine (Vitis vinifera L.): Focus on abscisic acid-mediated consequences on secondary metabolism and berry quality. Environmental and Experimental Botany 103, 138-147.

Fournier-Level A, Le Cunff L, Gomez C, Doligez A, Ageorges A, Roux C, ... This P. 2009. Quantitative genetic bases of anthocyanin variation in grape (Vitis vinifera L. subsp. sativa) berry: a quantitative trait locus to quantitative trait nucleotide integrated study. Genetics 183, 1127-1139.

Franks PJ, Beerling DJ. 2009. Maximum leaf conductance driven by CO_2 effects on stomatal size and density over geologic time. Proceedings of the National Academy of Sciences 106, 10343-10347.

Franks PJ, Doheny-Adams T, Britton-Harper ZJ, Gray JE. 2015. Increasing water-use efficiency directly through genetic manipulation of stomatal density. New Phytologist 207, 188-195.

Frioni T, Biagioni A, Squeri C, Tombesi S, Gatti M, Poni S. 2020. Grafting cv. Grechetto gentile vines to new m4 rootstock improves leaf gas exchange and water status as compared to commercial 1103p rootstock. Agronomy 10, 708.

Frioni T, Saracino S, Squeri C, Tombesi S, Palliotti A, Sabbatini P, ... Poni S. 2019. Understanding kaolin effects on grapevine leaf and whole-canopy physiology during water stress and re-watering. Journal of Plant Physiology 242, 153020.

Henry RJ. 2019. Innovations in plant genetics adapting agriculture to climate change. Current opinion in plant biology.

Hetherington AM, Woodward FI. 2003. The role of stomata in sensing and driving environmental change. Nature 424, 901-908.

Hughes J, Hepworth C, Dutton C, Dunn JA, Hunt L, Stephens J, ... Gray JE. 2017. Reducing stomatal density in barley improves drought tolerance without impacting on yield. Plant Physiology, 174, 776-787.

Jagadish SK, Way DA, Sharkey TD. 2021. Plant heat stress: concepts directing future research. Plant, cell & environment.

Kadir S. 2006. Thermostability of photosynthesis of Vitis aestivalis and V. vinifera. Journal of the American Society for Horticultural Science 131, 476-483.

Keller M, Romero P, Gohil H, Smithyman RP, Riley WR, Casassa LF, Harbertson, J. F. (2016). Deficit irrigation alters grapevine growth, physiology, and fruit microclimate. American Journal of Enology and Viticulture, 67(4), 426-435.

Lawson T, Blatt MR. (2014). Stomatal size, speed, and responsiveness impact on photosynthesis and water use efficiency. Plant physiology 164, 1556-1570.

Lawson T, McElwain JC. 2016. Evolutionary trade-offs in stomatal spacing. New Phytologist 210, 1149-1151.

Lawson T, Vialet-Chabrand S. 2019. Speedy stomata, photosynthesis and plant water use efficiency. New Phytologist 221, 93-98.

Lawson T, Craigon J, Black CR, Colls JJ, Landon G, Weyers JD. 2002. Impact of elevated CO_2 and O_3 on gas exchange parameters and epidermal characteristics in potato (Solanum tuberosum L.). Journal of Experimental Botany, 53, 737-746.

Lawson T, von Caemmerer S, Baroli I. 2010. Photosynthesis and stomatal behaviour. In Progress in botany 72 (pp. 265-304). Springer, Berlin, Heidelberg.

Levin AD, Matthews MA, Williams LE. 2020. Effect of Preveraison Water Deficits on the Yield Components of 15 Winegrape Cultivars. American Journal of Enology and Viticulture 71, 208-221.

Lu Z, Percy RG, Qualset CO, Zeiger E. 1998. Stomatal conductance predicts yields in irrigated Pima cotton and bread wheat grown at high temperatures. Journal of Experimental Botany 453-460.

Matthews JS, Vialet-Chabrand S, Lawson T. 2018. Acclimation to fluctuating light impacts the rapidity of response and diurnal rhythm of stomatal conductance. Plant Physiology 176, 1939-1951.

McAusland L, Vialet-Chabrand S, Davey P, Baker NR, Brendel O, Lawson T. 2016. Effects of kinetics of light-induced stomatal responses on photosynthesis and water-use efficiency. New Phytologist, 211, 1209-1220.

McDowell NG, White S, Pockman WT. 2008. Transpiration and stomatal conductance across a steep climate gradient in the southern Rocky Mountains. Ecohydrology: Ecosystems, Land and Water Process Interactions, Ecohydrogeomorphology 1, 193-204.

McElwain JC. 2004. Climate-independent paleoaltimetry using stomatal density in fossil leaves as a proxy for CO2 partial pressure. Geology 32, 1017-1020.

McElwain JC, Yiotis C, Lawson T. 2016. Using modern plant trait relationships between observed and theoretical maximum stomatal conductance and vein density to examine patterns of plant macroevolution. New Phytologist 209, 94-103.

Meinzer FC, Smith DD, Woodruff DR, Marias DE, McCulloh KA, Howard AR, Magedman AL. 2017. Stomatal kinetics and photosynthetic gas exchange along a continuum of isohydric to anisohydric regulation of plant water status. Plant, cell & environment 40, 1618-1628.

Merilo E, Yarmolinsky D, Jalakas P, Parik H, Tulva I, Rasulov B, ... Kollist H. 2018. Stomatal VPD response: there is more to the story than ABA. Plant Physiology,176, 851-864.

Meeus S, Van den Bulcke J, Wyffels F. (2020). From leaf to label: A robust automated workflow for stomata detection. Ecology and evolution, 10(17), 9178-9191.

Mosedale JR, Abernethy KE, Smart RE, Wilson RJ, Maclean IM. 2016. Climate change impacts and adaptive strategies: lessons from the grapevine. Global change biology 22, 3814-3828.

Ohsumi A, Kanemura T, Homma K, Horie T, Shiraiwa T. 2007. Genotypic variation of stomatal conductance in relation to stomatal density and length in rice (Oryza sativa L.). Plant Production Science 10, 322-328.

Pons A, Allamy L, Schüttler A, Rauhut D, Thibon C, Darriet P. 2017. What is the expected impact of climate change on wine aroma compounds and their precursors in grape?. OENO one 51, 141-146.

Poole I. Lawson T, Weyers JDB, Raven JA. 2000. Effect of elevated CO2 on the stomatal distribution and leaf physiology of Alnus glutinosa. New Phytologist 145, 511-521.

Qu M, Hamdani S, Li W, Wang S, Tang J, Chen Z, ... Zhu X. 2016. Rapid stomatal response to fluctuating light: an under-explored mechanism to improve drought tolerance in rice. Functional Plant Biology 43, 727-738.

Rogiers SY, Greer DH, Hutton RJ, Landsberg JJ 2009. Does night-time transpiration contribute to anisohydric behaviour in a Vitis vinifera cultivar?. Journal of Experimental Botany, 60, 3751-3763.

Romero P, Dodd IC, Martinez-Cutillas A. 2012. Contrasting physiological effects of partial root zone drying in field-grown grapevine (Vitis vinifera L. cv. Monastrell) according to total soil water availability. Journal of Experimental Botany 63, 4071-4083.

Sade N, Gebremedhin A, Moshelion M. 2012. Risk-taking plants: anisohydric behavior as a stress-resistance trait. Plant signaling & behavior 7, 767-770.

Senapati N, Brown HE, Semenov MA. 2019. Raising genetic yield potential in high productive countries: designing wheat ideotypes under climate change. Agricultural and forest meteorology 271, 33-45.

Soar CJ, Collins MJ, Sadras VO. 2009. Irrigated Shiraz vines (Vitis vinifera) upregulate gas exchange and maintain berry growth in response to short spells of high maximum temperature in the field. Functional Plant Biology 36, 801-814.

Soar CJ, Speirs J, Maffei SM, Penrose AB, McCarthy MG, Loveys BR. 2006. Grape vine varieties Shiraz and Grenache differ in their stomatal response to VPD: apparent links with ABA physiology and gene expression in leaf tissue. Australian journal of grape and wine research 12, 2-12.

Stevens J, Jones MA, Lawson T. 2021. Diverse Physiological and Physical Responses among Wild, Landrace and Elite Barley Varieties Point to Novel Breeding Opportunities. Agronomy 11, 921.

Tello J, Aguirrezábal R, Hernáiz S, Larreina B, Montemayor MI, Vaquero E, Ibáñez J. 2015. Multicultivar and multivariate study of the natural variation for grapevine bunch compactness. Australian journal of grape and wine research 21, 277-289.

van Bezouw RF, Keurentjes JJ, Harbinson J, Aarts MG. 2019. Converging phenomics and genomics to study natural variation in plant photosynthetic efficiency. The Plant Journal 97, 112-133.

Venios X, Korkas E, Nisiotou A, Banilas G. 2020. Grapevine Responses to Heat Stress and Global Warming. Plants 9, 1754.

Vialet-Chabrand S, Matthews JS, Simkin AJ, Raines CA, Lawson T. 2017. Importance of fluctuations in light on plant photosynthetic acclimation. Plant Physiology 173, 2163-2179

Zhang Q, Peng S, Li Y. 2019. Increase rate of light-induced stomatal conductance is related to stomatal size in the genus Oryza. Journal of Experimental Botany 70, 5259-5269.

Zhou Y, Massonnet M, Sanjak JS, Cantu D, Gaut BS. 2017. Evolutionary genomics of grape (Vitis vinifera ssp. vinifera) domestication. Proceedings of the National Academy of Sciences 114, 11715-11720.

Figure legends

Figure 1. Boxplots showing traits assessed during Experiment 1 (n=5 for 49 genotypes). Stomatal anatomical traits included stomatal density, stomatal size and anatomical g_{max}. Functional leaf traits included reduction in F_v/F_m under heat stress, carbon ($\delta^{13}C$) and nitrogen ($\delta^{15}N$) discrimination. Data were checked for normality and analysed with one-way ANOVA ($p<0.05$).

Figure 2. Correlation matrix for the traits analyzed in Experiment 1 (A), including r-value and significance (*** $p<0.001$, ** $p<0.01$, *$p<0.05$). Colors show positive or negative association. In B a scatter plot between average values of $\delta^{13}C$ and reduction in F_v/F_m is shown for the selected lines used for greenhouse experiment (Experiment 2). Data are means and genotypes are described in the figure. Light blue circle represent genotypes with low $_iWUE$ – HS tolerant while red circle represent high $_iWUE$ – HS sensitive respectively. Outsiders (i.e. genotypes with high $_iWUE$ and HS tolerant) are highlighted with black circle.

Figure 3. Stomatal anatomical traits assessed in Experiment 2 and for all the genotypes selected (n=5). A) Stomatal density, B) Stomata size and C) Anatomical g_{max}. Data were analyzed with one-way ANOVA (n=6) and different letters represent significant differences according to Fisher's test.

Figure 4. Steady-state traits estimated from step-changes analysis. A) stomatal conductance (g_{sat}); B) CO_2 assimilation rate at saturating light (A_{sat}); C) intrinsic water-sue efficiency calculated as A_{sat}/g_{sat} ($_iWUE$) and D) difference between g_{sat} and steady-state g_s at low light (δg_s). Data were analysed with one-way ANOVA (n=5) and different letters represent significant differences according to Fisher's test.

Figure 5. Dynamics of g_s and $_iWUE$ for all the genotypes subjected to a high to low light transition (A to F, 1000 to 100 µmol m^{-2} s^{-1} PPFD) and over 60 minutes. Data are means (n=3-6) ± standard error of the mean (SEM). In G, the modeled log decay function fitted for average g_s values of each genotype. In H, time to reach 50% of stomatal closure ($T50$) for each genotype and estimated with a log decay function. Data were analyzed with one-way ANOVA (n=5) and different letters represent significant differences according to Fisher's test.

Figure 6. A) Fitted log decay function for average g_s values of each genotype following a low to high VPD transition. B) Time to reach 50% of stomatal closure (T50) for each genotype and estimated with a log decay function (n=5). C) Steady state g_s at high VPD for each genotype. D) Limitation of A by g_s following a step-change in VPD (%). Data were analyzed with one-way ANOVA (n=3-4) different letters represent significant differences according to Fisher's test while in D data were analyzed with t-test.

Figure 7. Linear regression for field and greenhouse data and between time to reach 50% stomatal closure (T50) after a high to low light transition and $\delta^{13}C$ (A), intrinsic water use efficiency at saturating light and reduction in F_v/F_m compared to control under HS (B), time to reach 50% stomatal closure (T50) after a high to low light transition and reduction in F_v/F_m compared to control under HS (C), and gs after one hour at 3.5 kPa VPD and reduction in F_v/F_m compared to control under HS. Data points are individual values and lines were fitted with linear function in ggplot2. Coefficient of determination (r^2) is shown in the graphs and asterisks represent p-values ($p<0.05$*; $p<0.01$**).

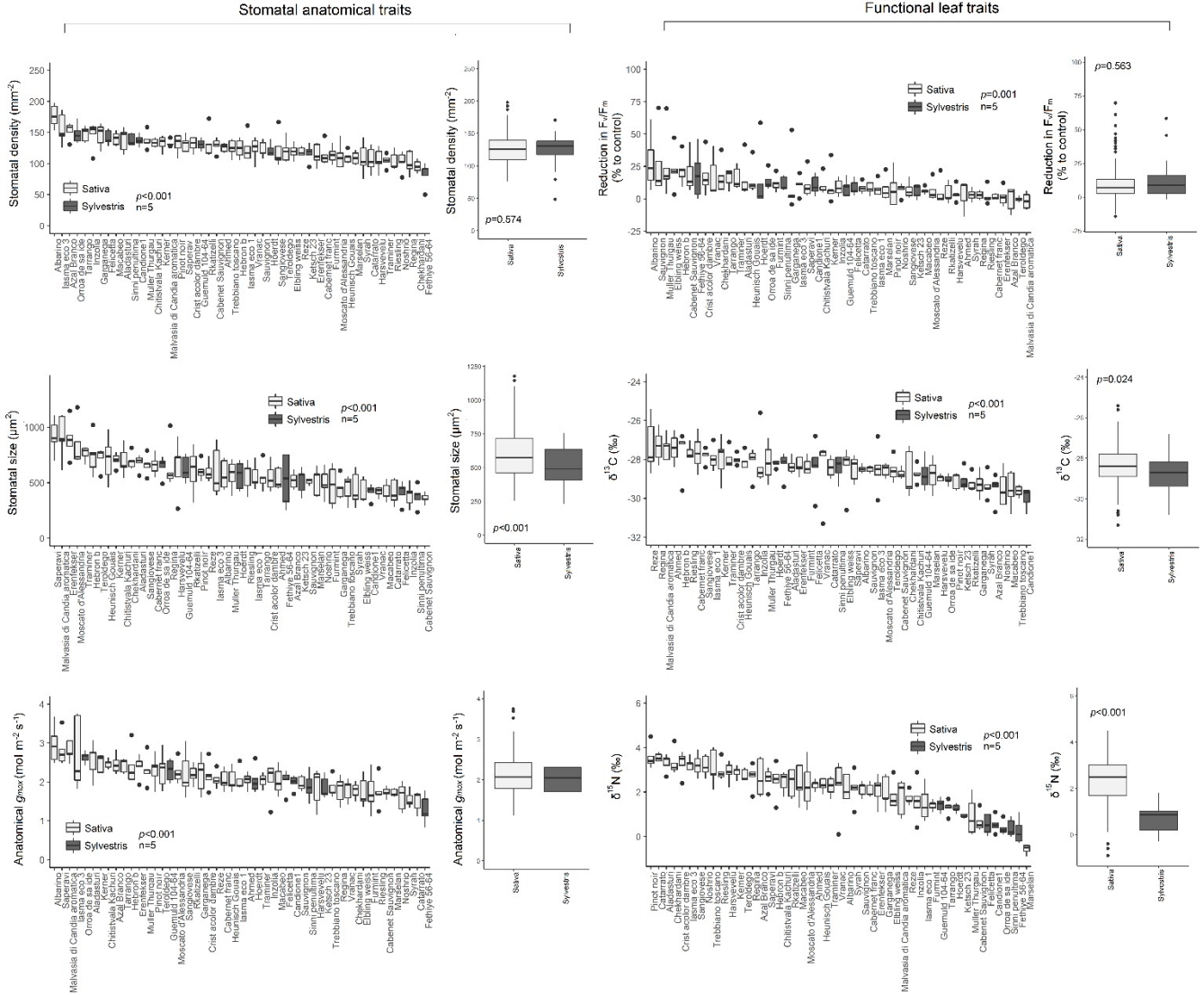

Figure 1. Boxplots showing traits assessed during Experiment 1 (n=5 for 49 genotypes). Stomatal anatomical traits included stomatal density, stomatal size and anatomical g_{max}. Functional leaf traits included reduction in F_v/F_m under heat stress, carbon ($\delta^{13}C$) and nitrogen ($\delta^{15}N$) discrimination. Data were checked for normality and analysed with one-way ANOVA ($p<0.05$).

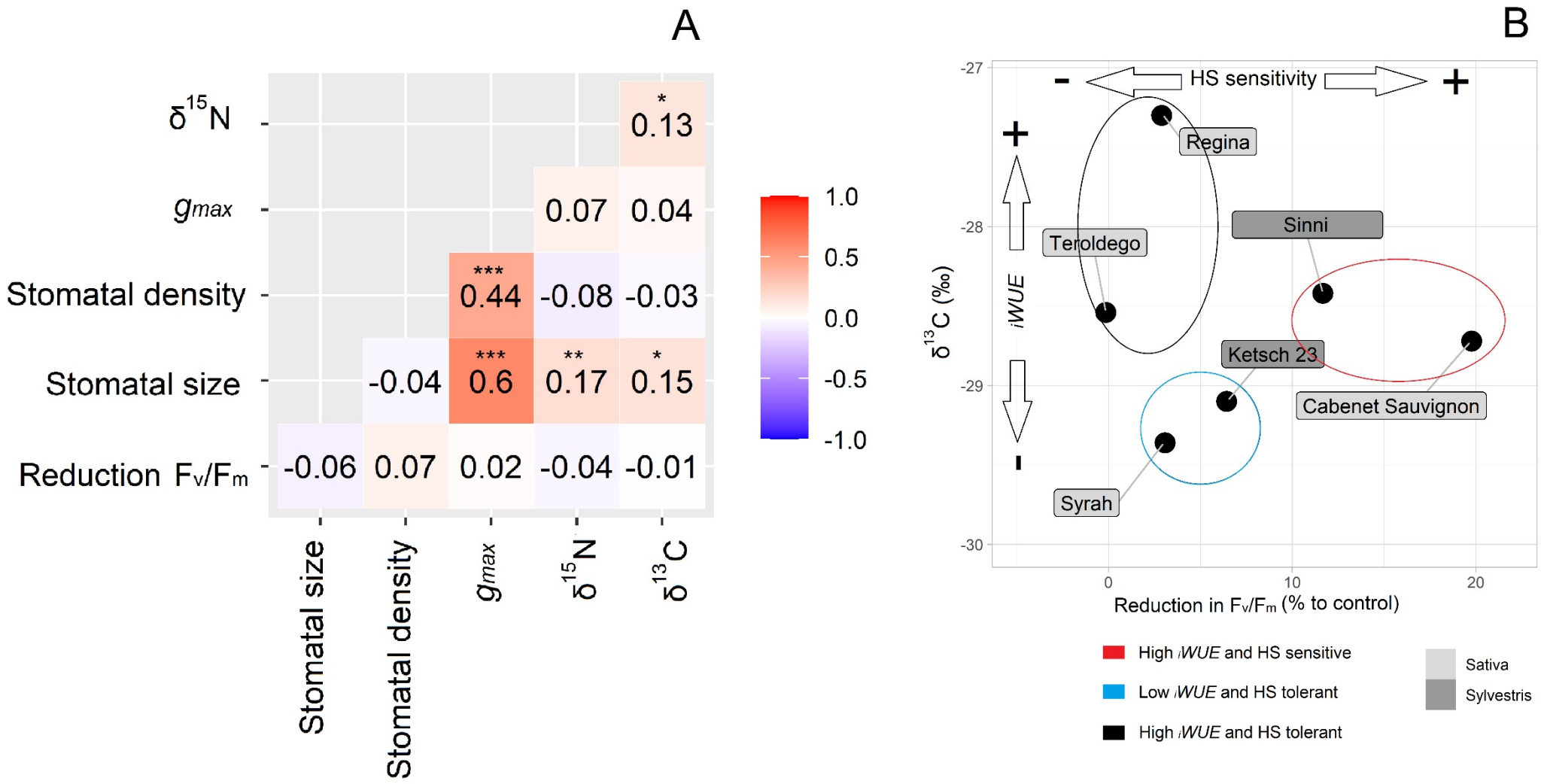

Figure 2. Correlation matrix for the traits analyzed in Experiment 1 (A), including r-value and significance (*** p<0.001, ** p<0.01, *p<0.05). Colors show positive or negative association. In B a scatter plot between average values of $\delta^{13}C$ and reduction in F_v/F_m is shown for the selected lines used for greenhouse experiment (Experiment 2). Data are means and genotypes are described in the figure. Light blue circle represent genotypes with low *iWUE* – HS tolerant while red circle represent high *iWUE* – HS sensitive respectively. Outsiders (i.e. genotypes with high *iWUE* and HS tolerant) are highlighted with black circle.

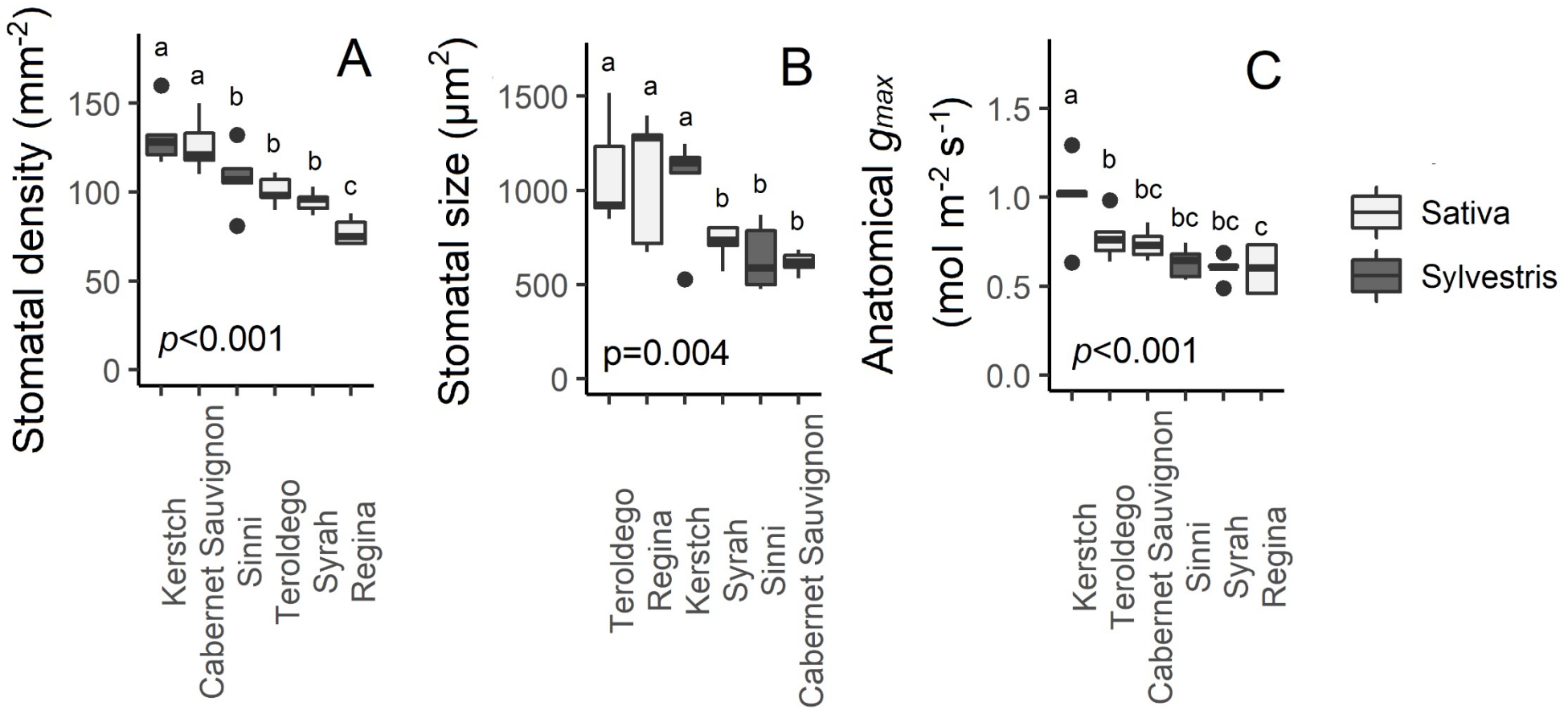

Figure 3. Stomatal anatomical traits assessed in Experiment 2 and for all the genotypes selected (n=5). A) Stomatal density, B) Stomata size and C) Anatomical g_{max}. Data were analyzed with one-way ANOVA (n=6) and different letters represent significant differences according to Fisher's test.

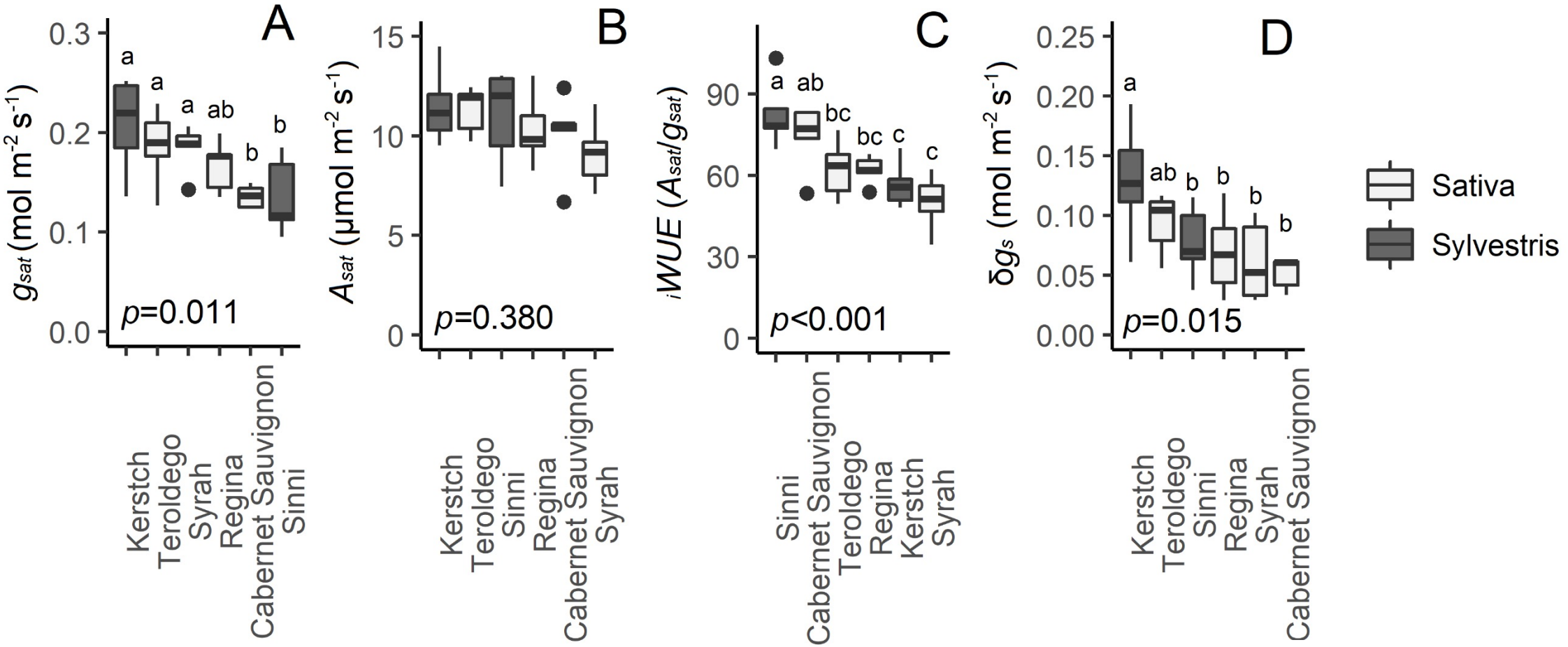

Figure 4. Steady-state traits estimated from step-changes analysis. A) stomatal conductance (g_{sat}); B) CO_2 assimilation rate at saturating light (A_{sat}); C) intrinsic water-sue efficiency calculated as A_{sat}/g_{sat} ($_{i}WUE$) and D) difference between g_{sat} and steady-state g_s at low light (δg_s). Data were analysed with one-way ANOVA (n=5) and different letters represent significant differences according to Fisher's test.

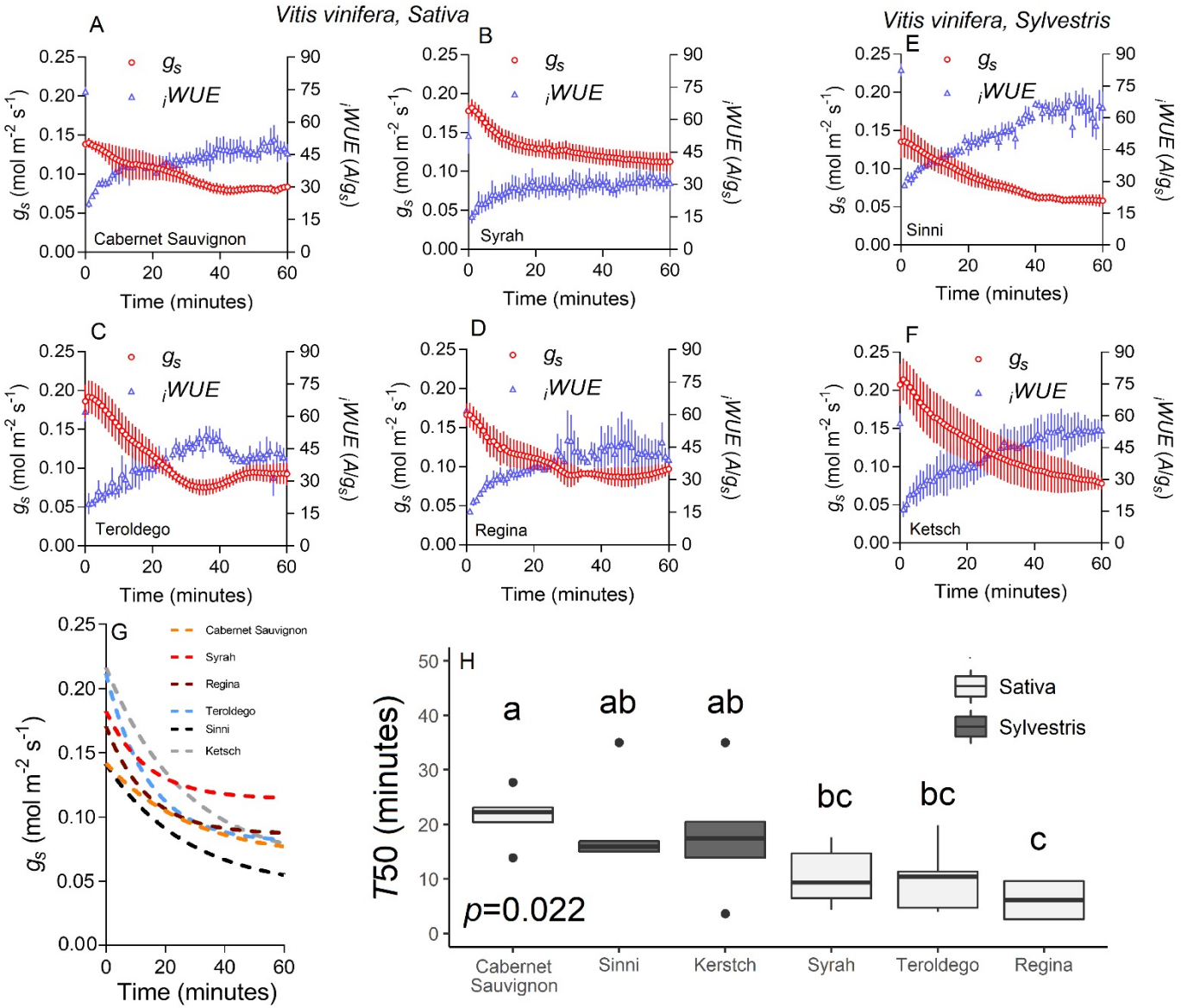

Figure 5. Dynamics of g_s and $_iWUE$ for all the genotypes subjected to a high to low light transition (A to F, 1000 to 100 µmol m^{-2} s^{-1} PPFD) and over 60 minutes. Data are means (n=3-6) ± standard error of the mean (SEM). In G, the modeled log decay function fitted for average g_s values of each genotype. In H, time to reach 50% of stomatal closure (*T*50) for each genotype and estimated with a log decay function. Data were analyzed with one-way ANOVA (n=5) and different letters represent significant differences according to Fisher's test.

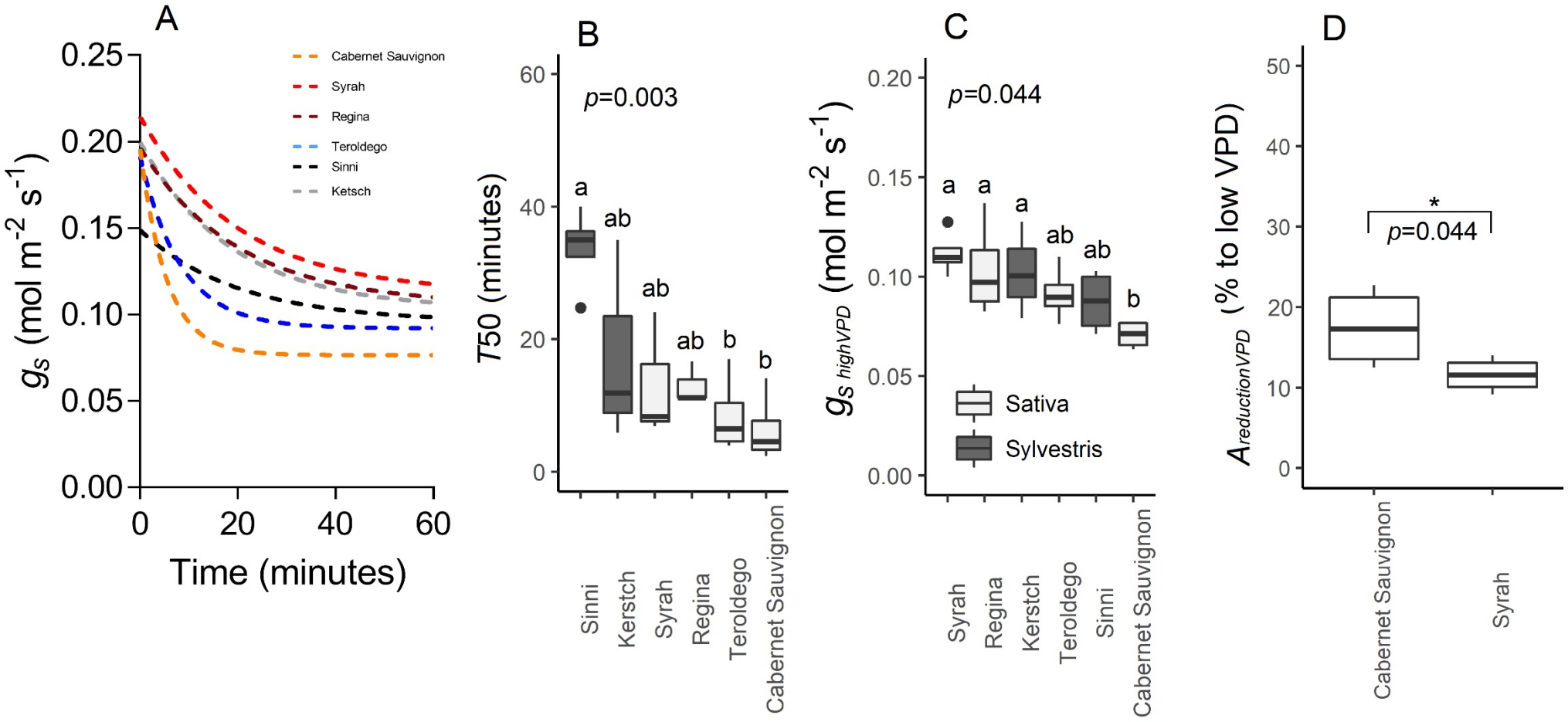

Figure 6. A) Fitted log decay function for average g_s values of each genotype following a low to high VPD transition. B) Time to reach 50% of stomatal closure (T50) for each genotype and estimated with a log decay function (n=5). C) Steady state g_s at high VPD for each genotype. D) Limitation of *A* by g_s following a step-change in VPD (%). Data were analyzed with one-way ANOVA (n=3-4) different letters represent significant differences according to Fisher's test while in D data were analyzed with t-test.

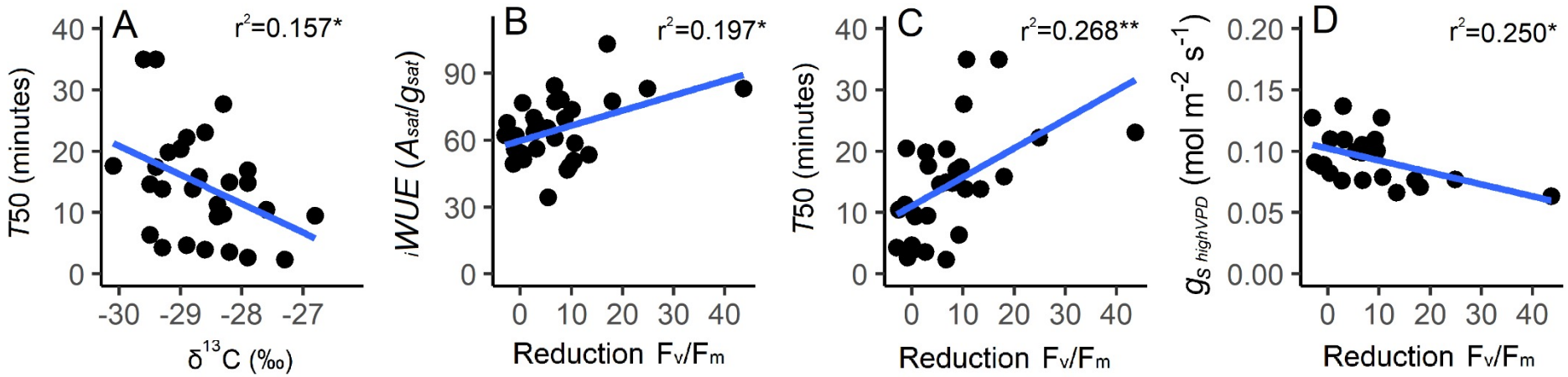

Figure 7. Linear regression for field and greenhouse data and between time to reach 50% stomatal closure (T50) after a high to low light transition and $\delta^{13}C$ (A), intrinsic water use efficiency at saturating light and reduction in F_v/F_m compared to control under HS (B), time to reach 50% stomatal closure (T50) after a high to low light transition and reduction in F_v/F_m compared to control under HS (C), and gs after one hour at 3.5 kPa VPD and reduction in F_v/F_m compared to control under HS. Data points are individual values and lines were fitted with linear function in ggplot2. Coefficient of determination (r^2) is shown in the graphs and asterisks represent p-values ($p<0.05$*; $p<0.01$**).